

Characteristic Studies of Synthesised Magnetite Fe₃O₄

Lai Lai Myo¹, Khin Ei Ei Thein², Cho Cho³

Abstract

In this research work, a magnetite Fe₃O₄ sample was synthesised by the magnetising reduction method. The raw material, hematite (Fe₂O₃), was reduced with various amounts of coke (0.12, 0.24 and 0.36 g) at reduction temperatures of 600, 700 and 800°C. According to the yield percent of synthesised samples, the optimum conditions were found to be 0.24 g (coke) and temperature at 700°C. The synthesised samples were characterised by XRD, SEM and FT IR analyses. The XRD results of M47 and M48 samples reduced at 700 and 800°C indicated the diffraction peaks correspond to the (2 2 0), (3 1 1), (4 0 0), (5 1 1) and (4 4 0) crystallographic orientations of the cubic phase of magnetite (Fe₃O₄) and the average crystallite sizes were 39.36 and 12.55 nm. SEM images showed that the morphologies of M47 and M48 samples were spherical in shape and partially aggregated structures. FT IR analysis of both samples revealed that the formation of the Fe-O bond was occurred at 555 and 542 cm⁻¹.

Keywords: hematite, coke, magnetite, magnetizing reduction method, crystallite size, morphologies

Introduction

Transition metal oxides have been of scientific and technological interest for many decades due to their interesting optical, magnetic, electrical and catalytical properties (Ozkaya *et al.*, 2009). Iron oxide particles (Fe₃O₄, Fe₂O₃, FeO) play a major role in many areas of chemistry, physics and material science. Magnetite Fe₃O₄ is one of the important magnetic iron oxide particles (Hariani *et al.*, 2013). It has extensive potential applications in various fields, such as biomedical applications, magnetic recording media, pigments, catalysis, environmental processes, information technology and many engineering applications (Takai *et al.*, 2019).

Magnetite (Fe₃O₄) is a black, ferromagnetic mineral containing both Fe²⁺ and Fe³⁺ in its crystal structure. The crystal structure of magnetite is inverse spinel with a unit cell consisting of 32 oxygen atoms in a face-centered cubic structure and a unit cell edge length of 0.839 nm. In this crystal structure, Fe²⁺ ions and half of the Fe³⁺ ions occupy octahedral sites and the other half of the Fe³⁺ occupies tetrahedral sites. Divalent iron atoms prefer to occupy octahedral sites to have a higher Crystal Field Stabilization Energy (CFSE), whilst the trivalent iron atoms have a CFSE=0 in both octahedral and tetrahedral sites (Kulkarni *et al.*, 2012).

The spinels can be described with general formula AB₂O₄, where A and B represent different oxidation states of the same cations, as in the case with magnetite, Fe₃O₄ (A = Fe²⁺, B = Fe³⁺). Depending on how cations occupy different interstices, spinel structure can be normal or inverse. In a normal spinel, the A cations occupy the tetrahedral interstitial sites and the B cations occupy the octahedral sites. In an inverse spinel, B cations occupy all of the tetrahedral and half of the octahedral sites, while the other species A occupy the remaining (half) of the octahedral sites (Redhammer and Tippelt, 2016).

¹ PhD candidate, Department of Chemistry, University of Yangon

² Associate Professor, Dr. Department of Chemistry, University of Yangon

³ Pro-Rector, Dr, University of Yangon

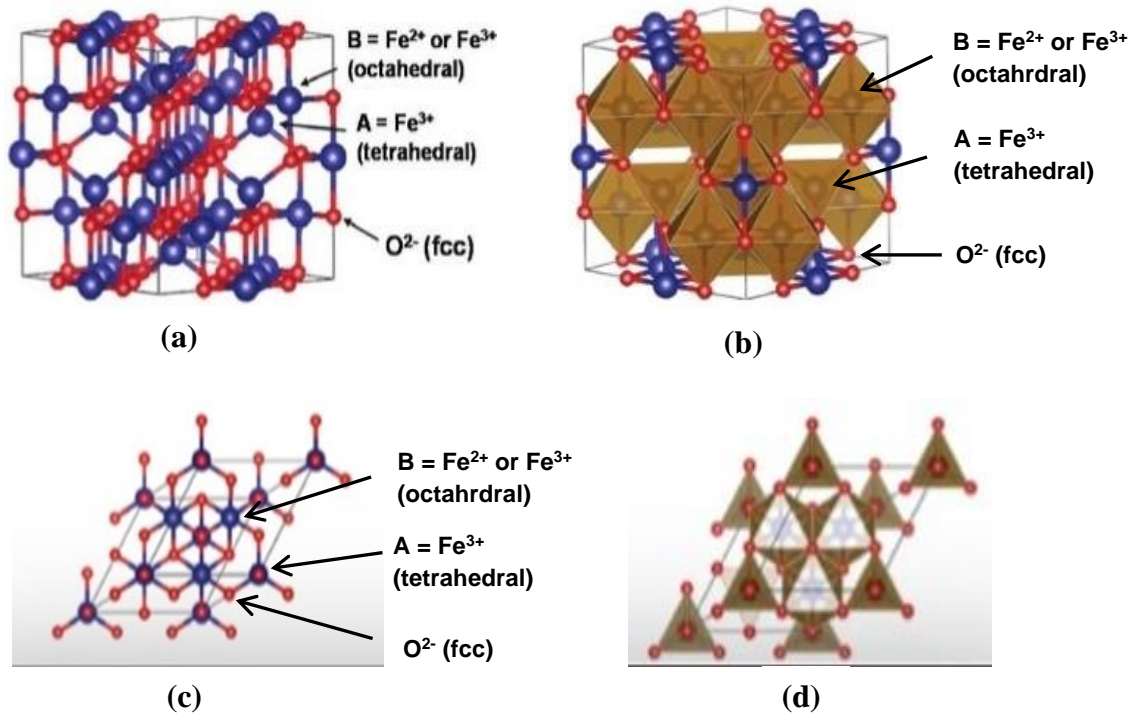


Figure 1. Schematic view of the inverse spinel crystal structure of magnetite (Fe₃O₄)

- (a) ball and stick model of the cubic unit cell
- (b) polyhedral model of the cubic unit cell (Unit-cell volume = 590.0196 Å³)
- (c) the rhombohedral primitive cell of Fe₃O₄
- (d) three-dimensional model of the rhombohedral primitive cell C, atoms at the apexes of the triangles lie in the same plane (Taimoory *et al.*, 2017).

Several methods have been developed for the preparation of magnetite Fe₃O₄ particles, such as hydrothermal or solvothermal method, sol-gel method, co-precipitation method, magnetizing reduction method and ball milling method. Among them, magnetizing reduction method has some advantages due to its simplicity, high product purity and low cost (Nor *et al.*, 2018). Magnetizing reduction, sometimes called magnetizing roast, is a process whereby weakly magnetic iron minerals (Fe₂O₃, FeCO₃ and FeS) can convert into strongly magnetic phase (Fe₃O₄). It can be readily performed at low operating costs and the product can be easily separated by external magnet. In order for the reduction to occur with sufficient velocity, 700°C appreciable quantities of heat are required. Coke, graphite, coal, char, deposited carbon and activated carbon can be used as reducing agents (Du *et al.*, 2017). A reduction goes from hematite (Fe₂O₃) to magnetite (Fe₃O₄) in which the reductant is mostly the CO gas. So, CO gas is produced by burning of carbon with oxygen (Moloto *et al.*, 2013). In this research work, magnetite Fe₃O₄ was synthesized from raw hematite ore by magnetizing reduction method and coke was used as the reducing agent in this process. The synthesized samples were characterized by XRD, SEM and FT IR analyses.

Materials and Methods

Sample Collection and Preparation

Raw material hematite (Fe_2O_3) ore was collected from Kya-Twin-Ye Village, Pyin Oo Lwin Township, Mandalay Region. The collected raw material was washed by distilled water to remove unwanted dust and impurities, dried in sunlight and crushed. Sieve size 80-125 μm was used to sieve the crushed raw material to obtain the uniform size. The reducing agent, coke was purchased from Academy Chemical Group, 28th Street, Pabedan Township, Yangon Myanmar.



Figure 2. Powdering process in raw hematite (Fe_2O_3)

Synthesis of Magnetite Fe_3O_4 Samples

The raw hematite (Fe_2O_3) powder and the reducing agent, coke were used to synthesise magnetite, Fe_3O_4 and the optimum conditions were also investigated by varying the amounts of reducing agent and reduction temperatures.

(1) Effect of the amounts of Reducing Agent on Reduction of Raw Hematite

4.791 g of raw hematite powder was mixed with various amounts of coke such as 0.12, 0.24 and 0.36 g, respectively and the mixtures were placed in each crucible. Before the reduction, the crucibles were covered with the lips to prevent oxidation reaction. And then, the mixtures were heated at 700°C in muffle furnace for 2 h and cooled to room temperature. The products were washed with deionized water and separated by using external magnet. The samples were dried at 70°C for 6 h. The obtained samples were denoted as M2, M4 and M6, respectively. Based on the yield percent, the sample (M4) was selected to investigate the optimum reduction temperature.

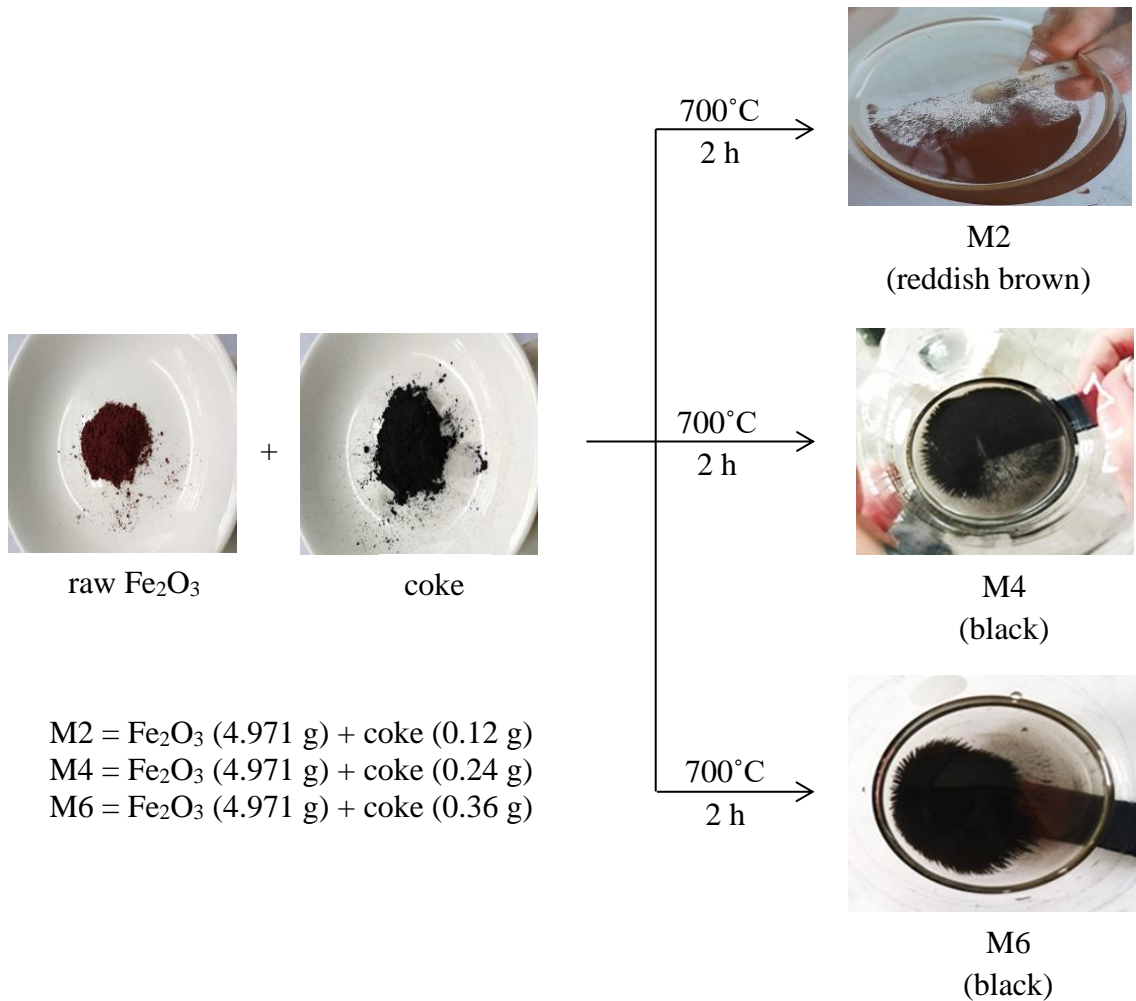


Figure 3. Effect of various amounts of reducing agent on raw hematite at 700°C

(2) Effect of the Reduction Temperature on Reduction of Raw Hematite

In the synthesis of magnetite, the reduction process was carried out as the same procedure described in above. From each reduction processes, the appropriate reaction time was 2 h and the amount of reducing agent was 0.24 g. Therefore, the other reduction processes were carried out by varying the reduction temperatures such as 600, 700 and 800°C. The synthesised samples were denoted as M46, M47 and M48 according to reduction temperatures of 600, 700 and 800°C, respectively.

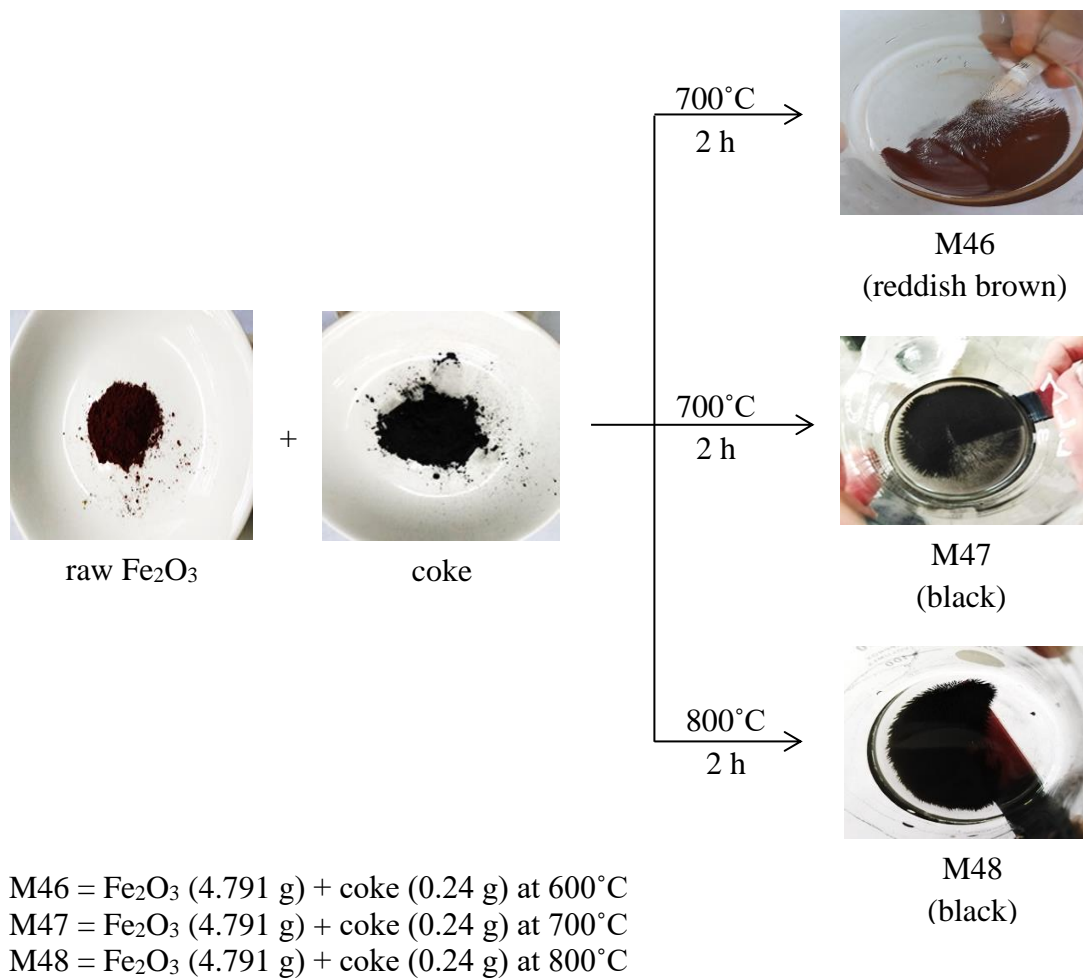


Figure 4. Effect of various temperature on raw hematite at 0.24 g coke

Results and Discussion

Yield Percent of Synthesised Magnetite Samples

The yield percent of synthesised samples are shown in Table 1 and Table 2. From the calculation of yield percent, sample (M47) was found to be the highest yield percent. According to yield percent of synthesised samples, the optimum conditions are amount of coke (0.24 g) and reduction temperature 700°C.

Table 1. Yield Percent of Synthesised Magnetite Samples with Various Amounts of Coke

Samples	Hematite : Amount of coke		Temperature (°C)	Yield of Magnetite (%)	Colour
	(g)	(g)			
M2	4.791	0.12	700	54.42	Reddish brown
M4	4.791	0.24	700	80.54	Black
M6	4.791	0.36	700	81.07	Black

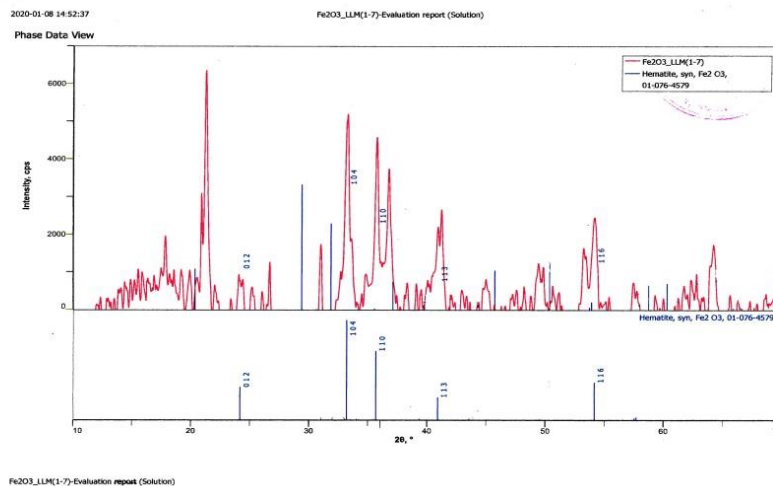
Table 2. Yield Percent of Synthesised Magnetite Samples at Different Temperatures

Samples	Hematite : Amount of coke		Temperature (°C)	Yield of Magnetite (%)	Colour
	(g)	(g)			
M46	4.791	0.24	600	66.01	Reddish brown
M47	4.791	0.24	700	80.54	Black
M48	4.791	0.24	800	74.35	Black

Characterization of Raw Hematite and Synthesised Magnetite

XRD Analysis of Raw Hematite

The phase identification and crystalline structures of raw hematite (Fe_2O_3) and synthesised magnetite (Fe_3O_4) samples were determined by XRD analysis. As shown in Figure 5, the XRD pattern of raw hematite (Fe_2O_3) indicated a series of diffraction peaks at 2θ of 24.67, 33.25, 36.00, 40.95 and 54.60 can be assigned to (0 1 2), (1 0 4), (1 1 0), (1 1 3) and (1 1 6) planes, respectively. The diffraction patterns were well matched with the literature (Fardood *et al.*, 2017). The impurities peaks were observed due to raw hematite.

Figure 5. XRD pattern of raw hematite (Fe_2O_3)

XRD Analysis of Synthesised Magnetite Samples

Figure 6 showed the XRD patterns of synthesised samples (M46, M47 and M48). According to XRD results of sample M46, the diffraction peaks at 2θ of 30.17, 35.68, 43.30, 57.38 and 63.56 can be assigned to (1 1 2), (1 2 1), (2 2 0), (0 3 3) and (4 0 0) planes. The diffraction peaks of sample M46 did not match with standard cubic structure of magnetite.

XRD results of sample M47 showed that the diffraction peaks corresponding to miller indices of (2 2 0), (3 1 1), (4 0 0), (5 1 1) and (4 4 0) were identical to the characteristic peaks of standard magnetite Fe_3O_4 with cubic structure.

XRD results of sample M48 indicated that the diffraction peaks corresponding to miller indices of (2 2 0), (3 1 1), (4 0 0), (5 1 1) and (4 4 0) were also identical to the characteristic peaks of standard magnetite Fe_3O_4 with cubic structure. Moreover, no characteristic peaks of impurities were detected in XRD patterns of M47 and M48 and only single phase of Fe_3O_4

were observed in both samples. The average crystallite sizes of synthesised samples were calculated by Debye Scherrer's formula. The results are shown in Table 5.

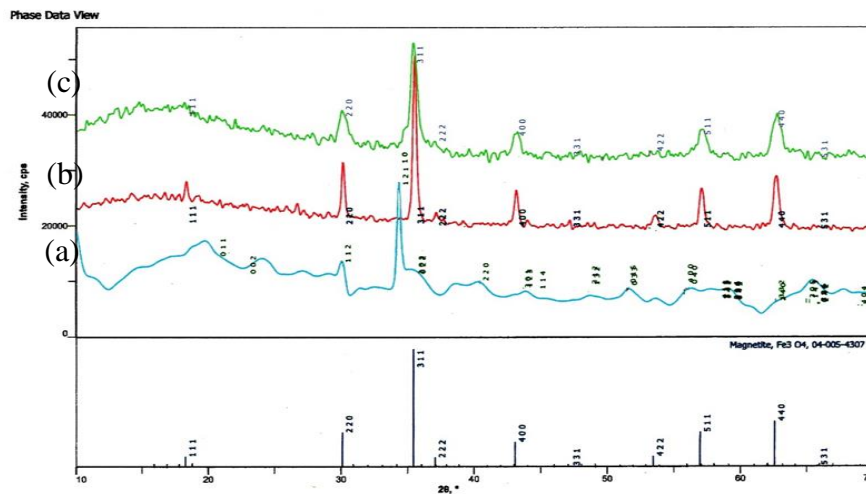


Figure 6. XRD patterns of magnetite samples (a) M46, (b) M47 and (c) M48

The XRD pattern of pure magnetite with standard cubic structure is also shown in Figure 7.

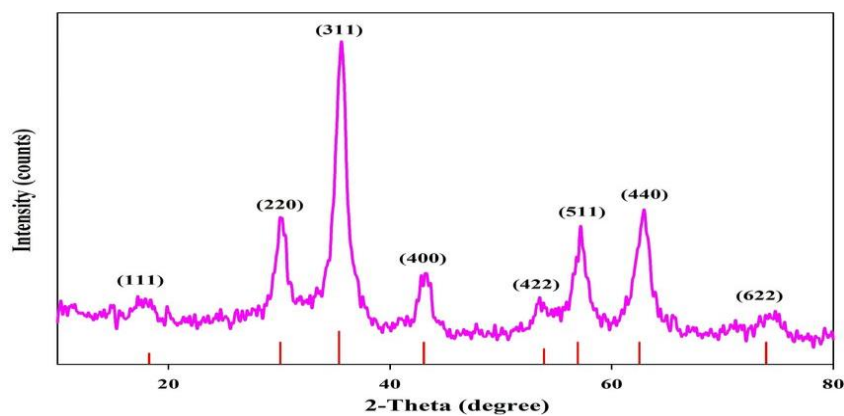


Figure 7. XRD pattern of pure magnetite (Hariani *et al.*, 2013)

Determination of Average Crystallite Sizes of Synthesised Magnetite Samples

The particle sizes of synthesised samples were determined using Debye Scherrer's formula. The results are shown in Table 5. The average crystallite size of M47 and M48 were 39.36 and 12.55 nm. According to XRD results, the lattice parameters of both synthesised samples were found to be 0.839 nm and 90° , which are well matched with reference data (Hariani *et al.*, 2013). Therefore, the crystal structures of synthesised samples M47 and M4 were cubic crystal structures.

Table 3. Miller Indices, Peak Position, FWHM and Average Crystallite Size of M47

No.	Miller Indices (h k l)	Peak Position (2θ)	FWHM	Crystallite Sizes (nm)
1	2 2 0	30.14	0.185	43.02
2	3 1 1	35.46	0.123	64.70
3	4 0 0	43.16	0.240	33.16
4	5 1 1	57.00	0.250	31.83
5	4 4 0	62.67	0.330	24.11
Average crystallite size				39.36

Table 4. Miller Indices, Peak Position, FWHM and Average Crystallite Size of M48

No.	Miller Indices (h k l)	Peak Position (2θ)	FWHM	Crystallite Sizes (nm)
1	2 2 0	30.15	0.603	12.63
2	3 1 1	35.51	0.510	15.60
3	4 0 0	43.23	0.520	15.30
4	5 1 1	57.16	0.810	9.85
5	4 4 0	62.74	0.850	9.39
Average crystallite size				12.55

Table 5. Average Crystallite Sizes of M46, M47 and M48 Samples

Sample	Average crystallite size (nm)	Crystal Structure
M46	-	-
M47	39.36	cubic
M48	12.55	cubic

Lattice parameter: Axial length, $a = b = c = 0.839$ nm

Interaxial angle, $\alpha = \beta = \gamma = 90^\circ$

SEM Analysis of Raw Hematite and Synthesised Magnetite Samples

The morphologies of raw hematite (Fe_2O_3) and magnetite (Fe_3O_4) samples were investigated by SEM. The microstructures of these samples were shown in Figure 8 (a), (b), (c) and (d). Figure 8 (a) and (b) showed the non-uniform distributed particles were observed in raw hematite (Fe_2O_3) and sample M46. In Figure 8 (c) and (d), the morphologies of M47 and M48 samples showed the spherical shape and some particles were aggregated.

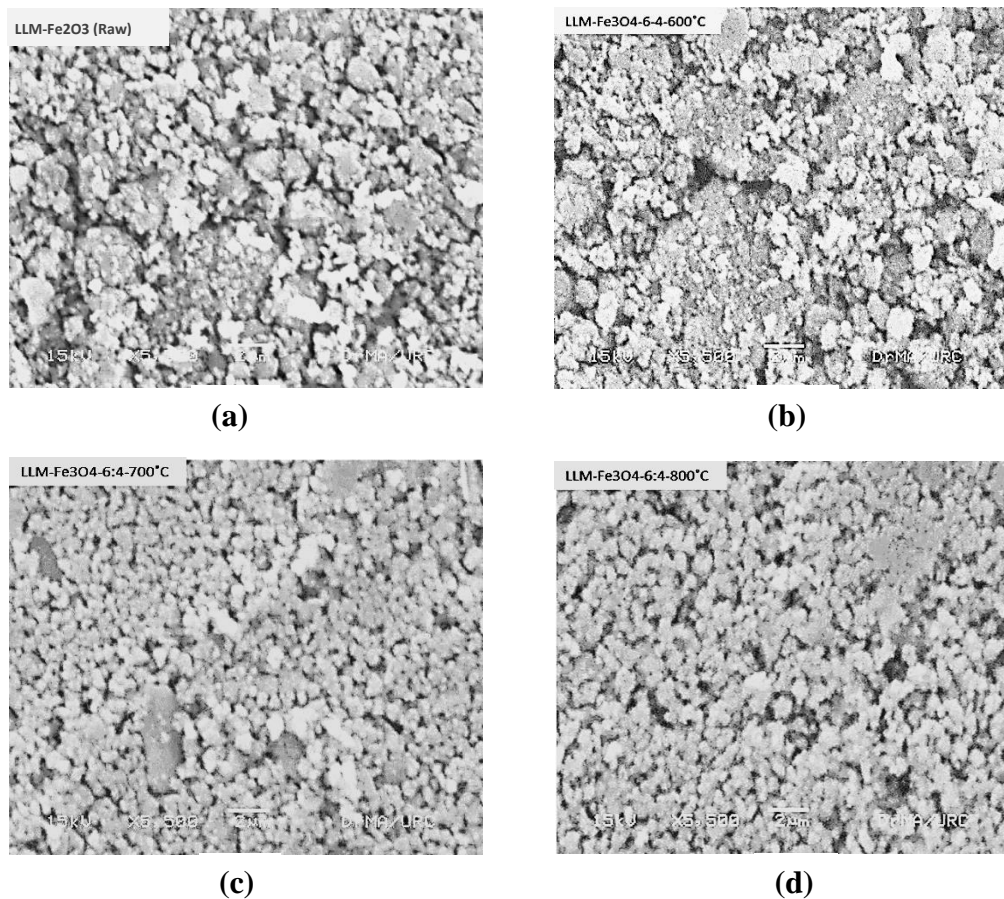


Figure 8. SEM micrographs of (a) raw hematite, (b) M46, (c) M47 and (d) M48

FT IR Analysis of Synthesised Magnetite Samples

FT IR spectroscopy was used to characterise the functional group analysis of synthesised magnetite samples. FT IR spectra of M47 and M48 samples were shown in Figure 9 and 10. In the FT IR spectrum of M47, the peak appeared at 3119 cm^{-1} was corresponded to O-H stretching vibration of water molecule adsorbed on sample surface (Castro *et al.*, 2009). The existence of peak at 1636 cm^{-1} was assigned to O-H bending vibration. The peaks found at 1405 and 1114 cm^{-1} in M47 were the stretching vibration of C-O group, where C-O group may be due to the effect of reductant CO gas (Mohammed, 2018). Moreover, the O-H bending bands at 891 and 793 cm^{-1} were assigned to vibrations in and out of plane, respectively (Castro *et al.*, 2009). Finally, the absorption peak observed at 555 cm^{-1} was the stretching vibration of Fe-O bond (Mohammed, 2018). The FT IR spectrum of M48 also showed the absorption peaks at 3029 cm^{-1} ($\nu_{\text{O-H}}$), 1401 cm^{-1} ($\nu_{\text{C-O}}$), 1087 cm^{-1} ($\nu_{\text{C-O}}$), 888 cm^{-1} ($\delta_{\text{O-H}}$), 793 cm^{-1} ($\delta_{\text{O-H}}$) and 542 cm^{-1} ($\nu_{\text{Fe-O}}$). The FT IR band assignments of M47 and M48 samples were shown in Table 6.

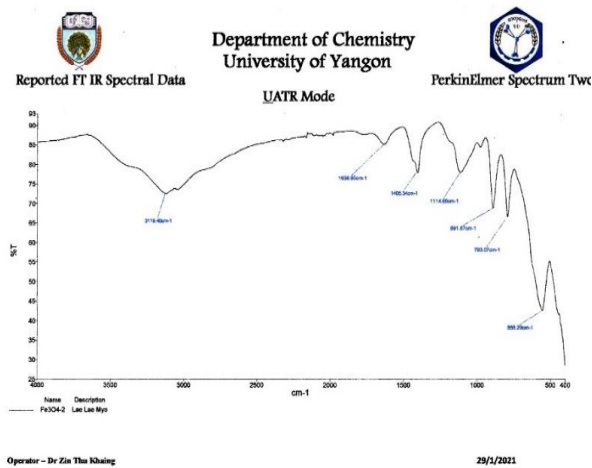


Figure 9. FT IR spectrum of magnetite sample M47

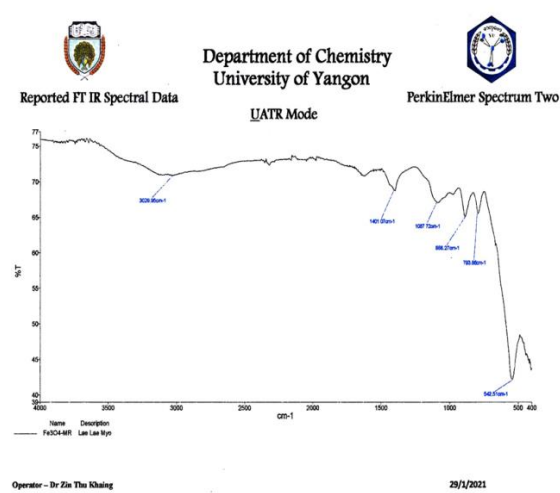


Figure 10. FT IR spectrum of magnetite sample M48

Table 6. Structural Assignments of Absorption Bands of M47 and M48 Samples

Samples	Observed wave number (cm ⁻¹)					
	ν _{O-H}	δ _{O-H}	ν _{C-O}	δ _{O-H}		ν _{Fe-O}
				(In plane)	(Out of plane)	
M47	3119	1636	1405 1114	891	793	555
M48	3029	-	1401 1087	888	793	542

Conclusion

Magnetite Fe₃O₄ samples were successfully synthesised by the magnetising reduction method using hematite as the raw material. The phase transformation, morphologies and functional group analysis of the synthesised samples were also studied by XRD, SEM and FT IR techniques. The XRD pattern of M46 indicated that the phase transformation from hematite to magnetite did not completely take place at 600°C. But the complete transformation was observed at 700 and 800°C for M47 and M48 according to XRD patterns. The average crystallite sizes were found to be 39.36 and 12.55 nm. The morphologies observed by SEM revealed that the iron oxide particles were more spherical and uniformly distributed with increasing reduction temperatures (700 and 800°C). The FT IR spectra of these magnetite samples (M47 and M48) revealed all the expected bands of interest, which are Fe-O stretching vibration modes at 555 and 542 cm⁻¹. In accordance with the overall results, magnetite Fe₃O₄ samples (M47 and M48) were successfully synthesised from raw hematite ore. Moreover, this method is simple and environmentally friendly without any toxic chemicals for the synthesis of magnetic Fe₃O₄ particles.

Acknowledgement

I would like to acknowledge to Rector Dr Tin Maung Tun, Pro-Rectors Dr Cho Cho and Dr Thida Aye, University of Yangon, for opportunity to submit this research paper. I also thanks to Dr Ni Ni Than, Professor and Head, Department of Chemistry, University of Yangon, for her kind advice and permission to allow this research paper. Thanks are also due to Universities' Research Centre (URC), University of Yangon.

References

- Castro, C. S., M. C. Guerreiro, M. Goncalves, L. C. A. Oliveira and A. S. Anastacio. (2009). "Activated Carbon/Iron Oxide Composites for the Removal of Atrazine from Aqueous Medium". *Journal of Hazardous Materials*, **164**, 609-614
- Du, W., S. Yang, F. Pan, J. Shangguan, J. Lu, S. Lui and H. Fan. (2017). "Hydrogen Reduction of Hematite Ore Fines to Magnetite Ore Fines at Low Temperatures". Hindawi, *Journal of Chemistry*, **3**, 1-11
- Fardood, S. T., A. Ramazani, Z. Golfar and S. W. Joo. (2017). "Green Synthesis of α -Fe₂O₃ (hematite) Nanoparticles using Tragacanth Gel". *Journal of Applied Chemical Research*, **11**(3), 19-27
- Hariani, P. L., M. Faizal, Ridwan, Marsi and D. Setiabudidaya. (2013). "Synthesis and Properties of Fe₃O₄ Nanoparticles by Co-precipitation Method to Removal Procion Dye". *International Journal of Environmental Science and Development*, **4**(3), 336-340
- Kulkarni, S. A., P. S. Sawadh and K. K. Kokate. (2012). "Synthesis and Characterization of Fe₃O₄ Nanoparticles for Engineering Applications". *International Conference on Benchmarks in Engineering Science and Technology*, **2**, 17-18
- Mohammed, S. M. H., (2018). "Characterization of Magnetite and Hematite Using Infrared Spectroscopy". *Journal of Engineering Sciences*, **2**(1), 38-44
- Moloto, L. H., S. S. Manzini and E. D. Dikio. (2013). "Reduction of Magnetite in the Presence of Activated Carbon Using Mechanical Alloying". *Journal of Chemistry*, **5**, 1-8
- Nor, W. F. K. W., S. K. C. Soh, A. A. A. R. Azmi, M. S. M. Yusof and M. Shamsuddin. (2018). "Synthesis and Physicochemical Properties of Magnetite Nanoparticles (Fe₃O₄) as Potential Solid Support for Homogeneous Catalysts". *Malaysian Journal of Analytical Science*, **22**(5), 768-774
- Ozkaya, T., M. S. Toprak, A. Baykal, H. Kavas, Y. Koseoglu and B. Aktas. (2009). "Synthesis of Fe₃O₄ Nanoparticles at 100 C and its Magnetic Characterization". *Journal of Alloys and Compounds*, **472**, 18-23
- Redhammer, G. J. and G. Tippelt. (2016). "Crystal Structure of Spinel-Type Li_{0.64} Fe_{2.15}Ge_{0.21}O₄". *Acta Cryst. E* **72**, 505-508
- Taimoory, S. M., J. F. Trant, A. Rahdar, M. Aliahmad, F. Sadeghfar and M. Hashemzaei. (2017). "Importance of the Inter-Electrode Distance for the Electrochemical Synthesis of Magnetite Nanoparticles: Synthesis, Characterization, Computational Modelling, and Cytotoxicity". *Journal of Surface Science and Nanotechnology*, **15**, 31-39
- Takai, Z. I., M. K. Mustafa, S. Asman and K. A. Sekak. (2019). "Preparation and Characterization of Magnetite (Fe₃O₄) Nanoparticles by Sol-Gel Method". *International Journal of Nanoelectronics and Materials*, **12**(1), 37-46

